

Original Investigation | OPTHALMIC MOLECULAR GENETICS

RYR1 Mutations as a Cause of Ophthalmoplegia, Facial Weakness, and Malignant Hyperthermia

Sherin Shaaban, MD, PhD; Leigh Ramos-Platt, MD; Floyd H. Gilles, MD; Wai-Man Chan, MS; Caroline Andrews, MS; Umberto De Girolami, MD; Joseph Demer, MD, PhD; Elizabeth C. Engle, MD

IMPORTANCE Total ophthalmoplegia can result from ryanodine receptor 1 (*RYR1*) mutations without overt associated skeletal myopathy. Patients carrying *RYR1* mutations are at high risk of developing malignant hyperthermia. Ophthalmologists should be familiar with these important clinical associations.

OBJECTIVE To determine the genetic cause of congenital ptosis, ophthalmoplegia, facial paralysis, and mild hypotonia segregating in 2 pedigrees diagnosed with atypical Moebius syndrome or congenital fibrosis of the extraocular muscles.

DESIGN, SETTING, AND PARTICIPANTS Clinical data including medical and family histories were collected at research laboratories at Boston Children's Hospital and Jules Stein Eye Institute (Engle and Demer labs) for affected and unaffected family members from 2 pedigrees in which patients presented with total ophthalmoplegia, facial weakness, and myopathy.

INTERVENTION Homozygosity mapping and whole-exome sequencing were conducted to identify causative mutations in affected family members. Histories, physical examinations, and clinical data were reviewed.

MAIN OUTCOME AND MEASURE Mutations in *RYR1*.

RESULTS Missense mutations resulting in 2 homozygous *RYR1* amino acid substitutions (E989G and R3772W) and 2 compound heterozygous *RYR1* substitutions (H283R and R3772W) were identified in a consanguineous and a nonconsanguineous pedigree, respectively. Orbital magnetic resonance imaging revealed marked hypoplasia of extraocular muscles and intraorbital cranial nerves. Skeletal muscle biopsy specimens revealed nonspecific myopathic changes. Clinically, the patients' ophthalmoplegia and facial weakness were far more significant than their hypotonia and limb weakness and were accompanied by an unrecognized susceptibility to malignant hyperthermia.

CONCLUSIONS AND RELEVANCE Affected children presenting with severe congenital ophthalmoplegia and facial weakness in the setting of only mild skeletal myopathy harbored recessive mutations in *RYR1*, encoding the ryanodine receptor 1, and were susceptible to malignant hyperthermia. While ophthalmoplegia occurs rarely in *RYR1*-related myopathies, these children were atypical because they lacked significant weakness, respiratory insufficiency, or scoliosis. *RYR1*-associated myopathies should be included in the differential diagnosis of congenital ophthalmoplegia and facial weakness, even without clinical skeletal myopathy. These patients should also be considered susceptible to malignant hyperthermia, a life-threatening anesthetic complication avoidable if anticipated presurgically.

JAMA Ophthalmol. 2013;131(12):1532-1540. doi:10.1001/jamaophthalmol.2013.4392
Published online October 3, 2013.

Author Affiliations: Author affiliations are listed at the end of this article.

Corresponding Author: Elizabeth C. Engle, MD, CLS14075, Boston Children's Hospital, 300 Longwood Ave, Boston, MA 02115 (elizabeth.engle@childrens.harvard.edu).

Section Editor: Janey L. Wiggs, MD, PhD.

The *RYR1* gene (OMIM 180901) on chromosome 19q13.1 encodes the skeletal muscle ryanodine receptor RYR1, the principal sarcoplasmic reticulum calcium release channel that plays a pivotal role in excitation-contraction coupling in muscle. Both recessive and dominant mutations in *RYR1* are increasingly recognized to cause a spectrum of congenital myopathies, including central core,¹⁻⁴ multimimicore,^{5,6} nemaline,⁷ and congenital fiber-type disproportion myopathy.⁸ Congenital ophthalmoplegia can segregate with *RYR1* mutations and, in particular, with multimimicore myopathy.^{9,10} Children with *RYR1* mutations and ophthalmoplegia typically have severe skeletal myopathy accompanied by respiratory insufficiency and develop scoliosis.^{6,11} Some *RYR1* mutations cause susceptibility to malignant hyperthermia,¹²⁻¹⁵ and ophthalmoplegia and malignant hyperthermia can also be coinherited.^{16,17}

We previously reported 3 children within a consanguineous pedigree with congenital bilateral complete ophthalmoplegia, facial diplegia, and only mild hypotonia, who had been diagnosed with atypical Moebius syndrome.¹⁸ Subsequently, we identified a nonconsanguineous pedigree in which 2 children have a similar phenotype and had been diagnosed with congenital fibrosis of extraocular muscles. Using next-generation exome sequencing, we identify recessive *RYR1* mutations in affected members of both families and also discover that these individuals are susceptible to malignant hyperthermia. These findings highlight the importance of recognizing *RYR1*-related myopathies in the differential diagnosis of congenital ophthalmoplegia and facial weakness.

Methods

Participants

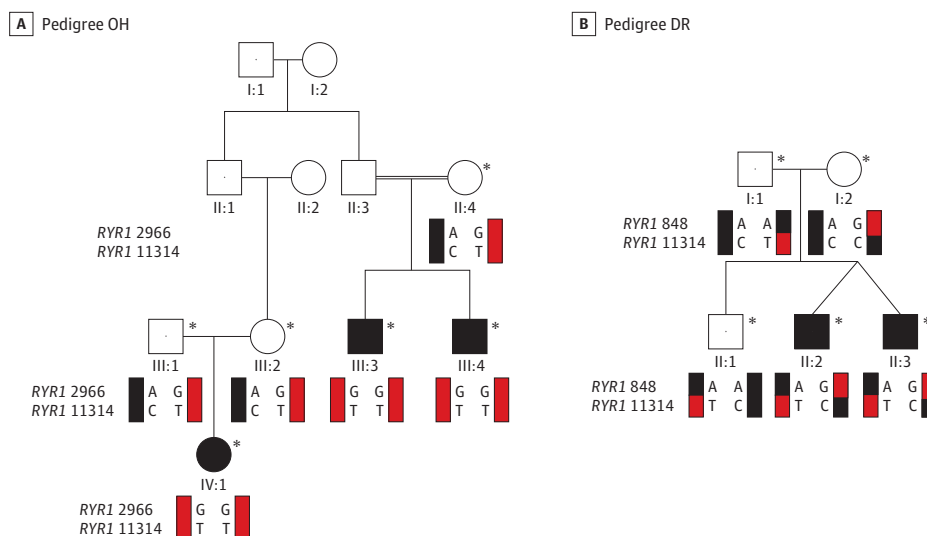
The study was approved by Boston Children's Hospital and University of California, Los Angeles institutional review boards. Written informed consent was obtained from participating family members or from their guardians. All investigations were conducted in accordance with the principles of the Declaration of Helsinki. Pedigree OH is a consanguineous pedigree of Mexican ethnicity (Figure 1A), and we previously reported the medical histories and ophthalmic examinations of the affected family members, III:3, III:4, and IV:1.¹⁸ Pedigree DR is a previously unreported nonconsanguineous pedigree of Portuguese origin with 2 affected children who are dizygotic twins (Figure 1B).

Mutation Identification in Pedigree OH

Homozygosity Mapping

To identify the genetic etiology for the clinical phenotype in pedigree OH, DNA was extracted from the peripheral blood of 3 affected family members (III:3, III:4, and IV:1) and 3 unaffected parents (II:4, III:1, and III:2) using the Puregene kit (Qiagen). Genotyping was performed using the GeneChip Human Mapping 10K Xba array (Affymetrix Inc)¹⁹ based on previously published protocols.²⁰ Given consanguinity in the family, we assumed a recessive mode of inheritance and predicted the causative variant would fall in a region of shared homozygosity. Homozygosity mapping was performed using Chip software.^{21,22}

Figure 1. Pedigree Structures of OH and DR



Schematic of pedigrees OH (A) and DR (B). Genotypes of *RYR1* variants c.2966A>G and c.11314C>T in pedigree OH and variants c.848A>G and c.11314C>T in pedigree DR are shown under genotyped family members; black schematic haplotype bars denote wild-type sequence, while red schematic haplotype bars denote mutant sequence. Note that the clinically unaffected parents in pedigree OH each harbor the same 2 *RYR1* mutations on 1 allele (red)

and have 1 wild-type allele (black). The clinically unaffected parents in pedigree DR each harbor a single, different *RYR1* mutation on 1 allele (half red and half black) and have 1 wild-type allele (black). Individual DR I:1 harbors the identical c.11314C>T mutation as 1 of the 2 mutations carried by individuals OH II:4, III:1, and III:2. *Those enrolled in the study. Circles indicate females; filled symbols, affected individuals; and squares, males.

Exome Capture and Sequencing, Read Mapping, and Variant Annotation

We performed whole-exome sequencing on DNA from individuals III:3, III:4, and IV:1. Three micrograms of genomic DNA were processed with the SureSelect Human All Exon Kit version 1 (Agilent Technologies).²³ Captured libraries were sequenced on a HiScanSQ (Illumina).²⁴ After sequencing, high-quality reads were aligned to the human reference genome sequence (UCSC hg18, NCBI build 36.1) via the ELAND version 2 program (Illumina). Variant calling of single-nucleotide polymorphisms (SNPs) and insertions/deletions (indels) was done with CASAVA software (Illumina).

Data Analysis and Mutation Identification

The ANNOVAR annotation package²⁵ was used for variant annotation. Polymorphisms were excluded by filtering high-quality variants against dbSNP130²⁶ and 1000 Genomes Project²⁷ data as well as by excluding variants with more than 1% frequency in the Exome Variant Server, NHLBI Exome Sequencing Project (<http://evs.gs.washington.edu/EVS/>). Only novel coding splice site, missense, and nonsense variants and indels were retained for final variant analysis. Prediction of functional consequences of nonsynonymous mutations was done using the SIFT,²⁸ PolyPhen-2,²⁹ and Pmut³⁰ algorithms. Putative mutations were then confirmed and segregation with affection status was tested among family members using Sanger sequencing.

Mutation Identification in Pedigree DR

Whole-exome sequencing was performed on a DNA sample from the affected individual DR II:2. Three micrograms of genomic DNA were processed with the SureSelect Human All Exon Kit version 4 plus untranslated regions. Captured libraries were sequenced on a HiSeq 2000 (Illumina). High-quality reads were aligned to the human reference genome sequence (UCSC hg19, NCBI build 37.1) via the Burrows-Wheeler Aligner program.³¹ Variant calling of SNPs and indels was done using SAMtools.³² Resulting data were analyzed assuming recessive inheritance where both homozygous and compound heterozygous variants were investigated. The methods described earlier for mutation identification and to confirm segregation were followed.

Clinical, Radiological, and Pathological Assessment

Following analysis of the genetic results, 11-year-old individual OH IV:1 underwent confirmatory clinical diagnostic DNA testing and a battery of clinical procedures including muscle biopsy, electromyography, nerve conduction velocity, electrocardiography, pulmonary function tests, and blood and cerebrospinal fluid analyses. Available medical histories of the other 2 affected individuals in pedigree OH were reviewed.

Full ophthalmic and neurological examinations were conducted when individuals DR II:2 and DR II:3 were 8 months old. Individual DR II:2 had had cytogenetic analysis and underwent real-time sonographic imaging and nonenhanced computerized tomography of the brain, as well as magnetic described.¹⁸ Their available subsequent medical histories were reviewed.

Muscle specimens from individuals OH IV:1 and DR II:2 were obtained for clinical diagnostic studies from the quadriceps muscle under local anesthesia. Specimens were frozen immediately in isopentane-cooled liquid nitrogen and stored at -80°C . Sections of fresh frozen muscle were stained for hematoxylin-eosin, modified trichrome, myofibrillar adenosine triphosphatase at pH 4.3, 4.6, and 9.4, periodic acid-Schiff (without and with diastase), Oil Red O, nicotinamide adenine dinucleotide dehydrogenase-tetrazolium reductase, succinic dehydrogenase, cytochrome-*c* oxidase, alkaline phosphatase, and acid phosphatase. Samples for electron microscopy were fixed in glutaraldehyde, 5%, and osmium tetroxide, 1%, in 0.1M cacodylate buffer.

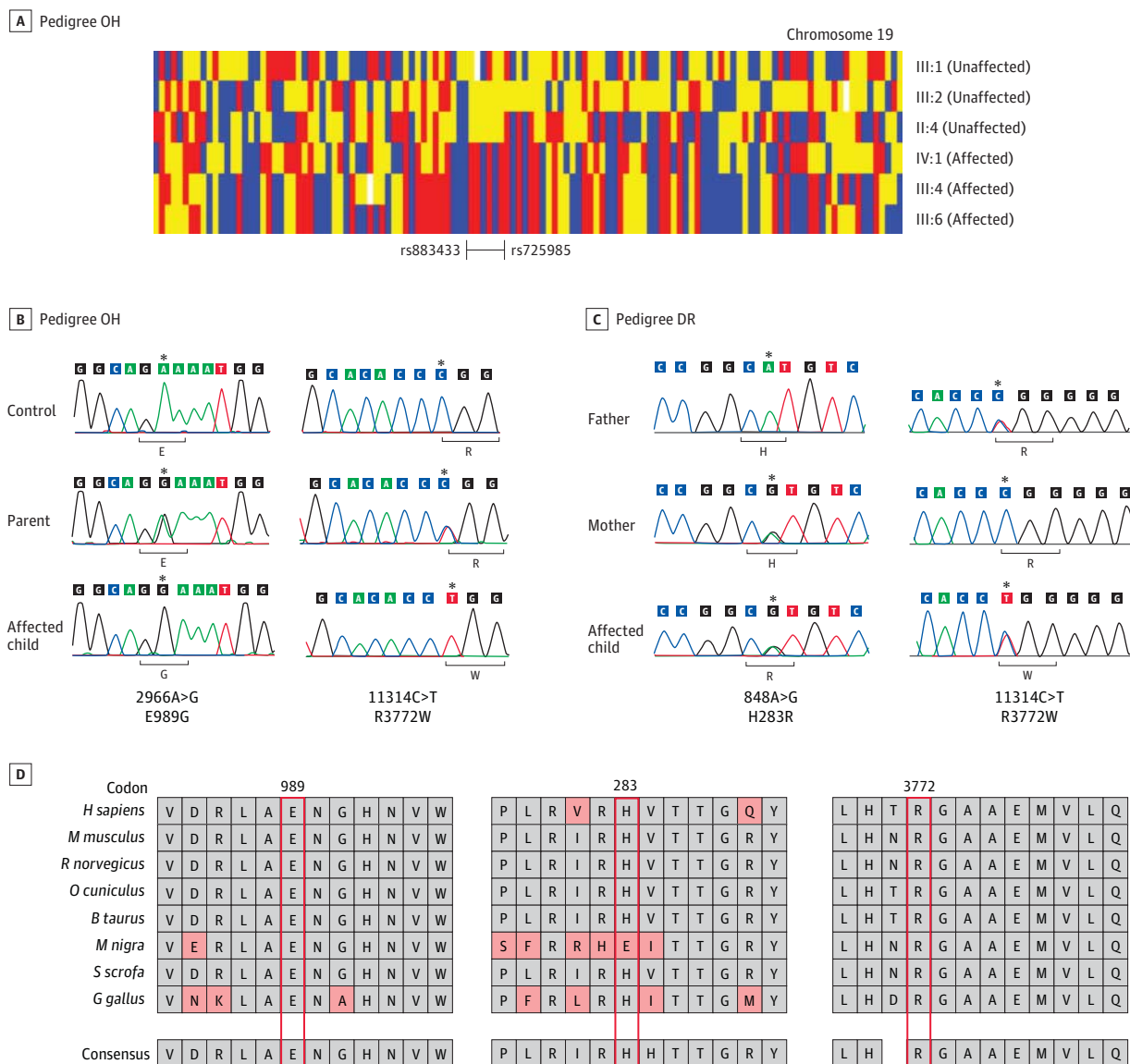
Results

Genetic Analysis

Homozygosity mapping in pedigree OH revealed only 1 homozygous region greater than 2 Mb that was shared among the 3 affected individuals and not the unaffected parents. This approximately 3-Mb region on chromosome 19q13.12-19q13.2 was flanked by markers rs725985 and rs883433 (Figure 2A). Because there were more than 150 genes in the region, we proceeded with whole-exome sequencing for causative variant identification. We obtained mean coverage of 88% at $\times 10$ resulting in approximately 18 000 exonic variants in each sample. Because we hypothesized a recessive mode of inheritance, we investigated the homozygous novel variants falling within the shared region of homozygosity (19q13.12-19q13.2) that were not in the dbSNP, 1000 Genomes, or Exome Variant Server databases. This analysis resulted in only 2 homozygous missense variants, both of which fell within the *RYR1* gene (c.2966A>G; p.E989G and c.11314C>T; p.R3772W) (Table). Both residues are highly conserved (Figure 2D) and in silico analysis predicted both to be damaging. Both variants were absent from control DNA samples and segregated with affection status; unaffected parents were heterozygous and the affected individuals were homozygous for the mutant alleles (Figure 2B). Neither of the mutations fell in any of the dominant “hot-spot” regions of *RYR1* mutations, consistent with previously reported recessive *RYR1* mutations that appear to alter residues anywhere along the length of RYR1 protein.³³

On identification of *RYR1* mutations in pedigree OH, we reviewed the cohort of families referred to us with ophthalmoplegia and facial weakness and identified a second pedigree, DR, with a phenotype similar to pedigree OH. We hypothesized that *RYR1* mutations could also be causative in this pedigree, and because the *RYR1* gene is a very large gene encoded by 106 exons, we performed whole-exome sequencing on affected individual DR II:2 and targeted our sequence analysis to the *RYR1* gene. We obtained an average coverage of more than 95% at $\times 10$ resulting in 23 236 exonic variants. Data were analyzed as described for pedigree OH except, because of the absence of consanguinity, we assumed a compound heterozygous model of inheritance. We identified 2 heterozygous *RYR1* missense mutations, a novel c. 848A>G; p.H283R that falls in the first *RYR1* hot-spot mutation region and the recurrent mutation c.11314C>T;

Figure 2. Homozygosity Mapping and Mutation Analysis



A, Schematic showing regions of shared homozygosity on chromosome 19 in pedigree OH created by genotypes from individuals III:1, III:2, II:4, IV:1, III:4, and III:6 by dChip software.²² Red or blue denotes homozygous AA or BB, yellow denotes heterozygous AB, and white denotes absent call. The homozygous region shared by the 3 affected children and no parent is bordered by single-nucleotide markers rs725985 and rs883433. B, Sanger sequencing chromatograms from an unrelated control individual (top), unaffected parent (middle), and affected child (bottom) of pedigree OH. The parent is heterozygous and the affected children are homozygous for *RYR1* c.2966A>G (left) and *RYR1* c.11314C>T (right) nucleotide substitutions. The wild-type and predicted amino acid substitutions are provided below each sequence. Asterisks indicate the bases where the mutation occurred. C, Sanger

sequencing chromatograms from an unaffected father (top), unaffected mother (middle), and affected child (bottom) of pedigree DR. The father has a wild-type sequence at *RYR1* c.848 and a heterozygous *RYR1* 11314C>T nucleotide substitution, and the mother has a heterozygous *RYR1* 848A>G nucleotide substitution and is wild-type at *RYR1* c.11314. The affected child is heterozygous at both nucleotides. The wild-type and predicted amino acid substitutions are provided below each sequence. D, Evolutionary conservation of *RYR1* glutamic acid 989, histidine 283, and arginine 3772 residues in 8 species. *B taurus* indicates *Bos taurus*; *G gallus*, *Gallus gallus*; *H sapiens*, *homo sapiens*; *M musculus*, *Mus musculus*; *M nigra*, *Macaca nigra*; *O cuniculus*, *Oryctolagus cuniculus*; *R norvegicus*, *Rattus norvegicus*; and *S scrofa*, *Sus scrofa*.

p.R3772W (Figure 2C). Neither variant existed in any of the common databases or were present in control individuals, both were predicted to be damaging, both altered highly conserved residues, and segregation analysis confirmed that 1 mutation was inherited from each parent. The unaffected sibling DR II:1 carried the heterozygous missense c. 11314C>T mutation (Figure 2C).

Clinical Assessments

Pedigree OH

As previously reported,¹⁸ the 3 affected members of pedigree OH had normal gestational and birth histories and were born full term. Each had congenital complete ophthalmoplegia. At near central gaze, individual OH III:3 had exotropia of 18 prism

Table. Exome Sequence Data (Pedigree OH)

	Individual		
	OH III:3	OH III:4	OH IV:1
% of Coverage at $\times 10$	91	84	89.9
No. of total SNPs	18 494	17 115	18 662
No. of novel SNPs	1302	1098	632
(+) No. of pathogenic variants	921	725	471
(+) No. of homozygous variants	60	120	42
(+) No. of chromosome 19q13.12-19q13.2 variants	3	2	3
(+) No. of variants shared by other 2 affected individuals	2	2	2

Abbreviation: SNP, single-nucleotide polymorphism.

diopters (Δ), individual OH III:4 had exotropia of 18 Δ and 10 Δ hypertropia, and individual OH IV:1 showed alignment between orthotropia to 10 Δ exotropia. All 3 children had in addition bilateral ptosis and bilateral facial diplegia, while hypotonia was reported for individuals III:3 and IV:1. Magnetic resonance imaging of the affected children had revealed apically narrowed bony orbits, marked extraocular muscle hypoplasia, abnormally small motor nerves within the orbit, yet normal-appearing brainstems and subarachnoid portions of the cranial nerves innervating the extraocular muscles.¹⁸ The children were diagnosed with atypical Moebius syndrome.

The proband, IV:1, underwent additional clinical evaluations at age 11 years. Intellectual and social development were normal. She had nonprogressive complete ophthalmoplegia, ptosis, and facial weakness. She had mild hypotonia, deep tendon reflexes were grade +1, and she had normal axial and limb muscle strength apart from weak ankle dorsiflexion. She had ankle contractures and toe-walked; otherwise, her gait was normal. Sensory examination and coordination were normal and she had no history of respiratory compromise or scoliosis. Nerve conduction velocity and repetitive nerve stimulation were normal, while electromyography revealed decreased motor unit duration and early recruitment in the anterior tibialis consistent with a myopathic process. Electrocardiography and echocardiography were normal while pulmonary function tests showed a low maximum expiratory pressure. Creatine kinase levels were normal. Tests for metabolic and mitochondrial diseases including genetic screening were found to be normal except for low free and total carnitine levels. Individual IV:1 was receiving carnitine and vitamin supplements and physiotherapy for her ankle contractures.

Review of the intervening medical histories of her 2 affected cousins revealed nonprogressive ophthalmoplegia, ptosis and facial weakness, mild hypotonia, and grade 1+ deep tendon reflexes, with normal sensory testing. Individual III:3 had a history of delayed motor milestones. Individual III:4 had undergone an emergency surgery for a ruptured appendix, complicated by malignant hyperthermia requiring hospitalization with intensive care for 2 weeks.

Pedigree DR

The dizygotic twins were born full term following a pregnancy remarkable only for in vitro fertilization. The first twin was born vaginally and the second required cesarean section. Both infants had severe neonatal hypotonia and axial weakness. When examined at 8 months of age, tone and muscle strength had im-

proved significantly since birth, but they remained hypotonic; both boys could sit without support for 30 seconds and could pull to stand. They had complete ophthalmoplegia with 16 Δ exotropia in central gaze at near, bilateral ptosis, and facial weakness. Deep tendon reflexes were grade 2+ and symmetric, with no pathological reflexes. At age 12 years, intellectual and social development were normal. Ophthalmoplegia and facial weakness were unchanged, and both boys had been diagnosed with congenital fibrosis of extraocular muscles and undergone ptosis surgery. Inability to fully close their eyes led to drying and corneal perforation in 1 twin, requiring corneal transplant. Both boys had difficulties with chewing and swallowing. Both boys had absent patellar reflexes, yet muscle tone was only mildly decreased in one and normal in the other. Neither boy had respiratory compromise or scoliosis. Laboratory and genetic investigations revealed no metabolic or mitochondrial abnormalities. High-resolution magnetic resonance imaging of the orbit performed for individual DR II:2 at 8 months of age revealed atrophy of extraocular muscles with intramuscular fat; the inferior rectus muscles were partially spared. The posterior halves of the superior oblique muscles were more affected than their anterior halves. The intraorbital nerves to the extraocular muscles were thin and appeared hypoplastic while the optic nerve appeared normal (Figure 3).

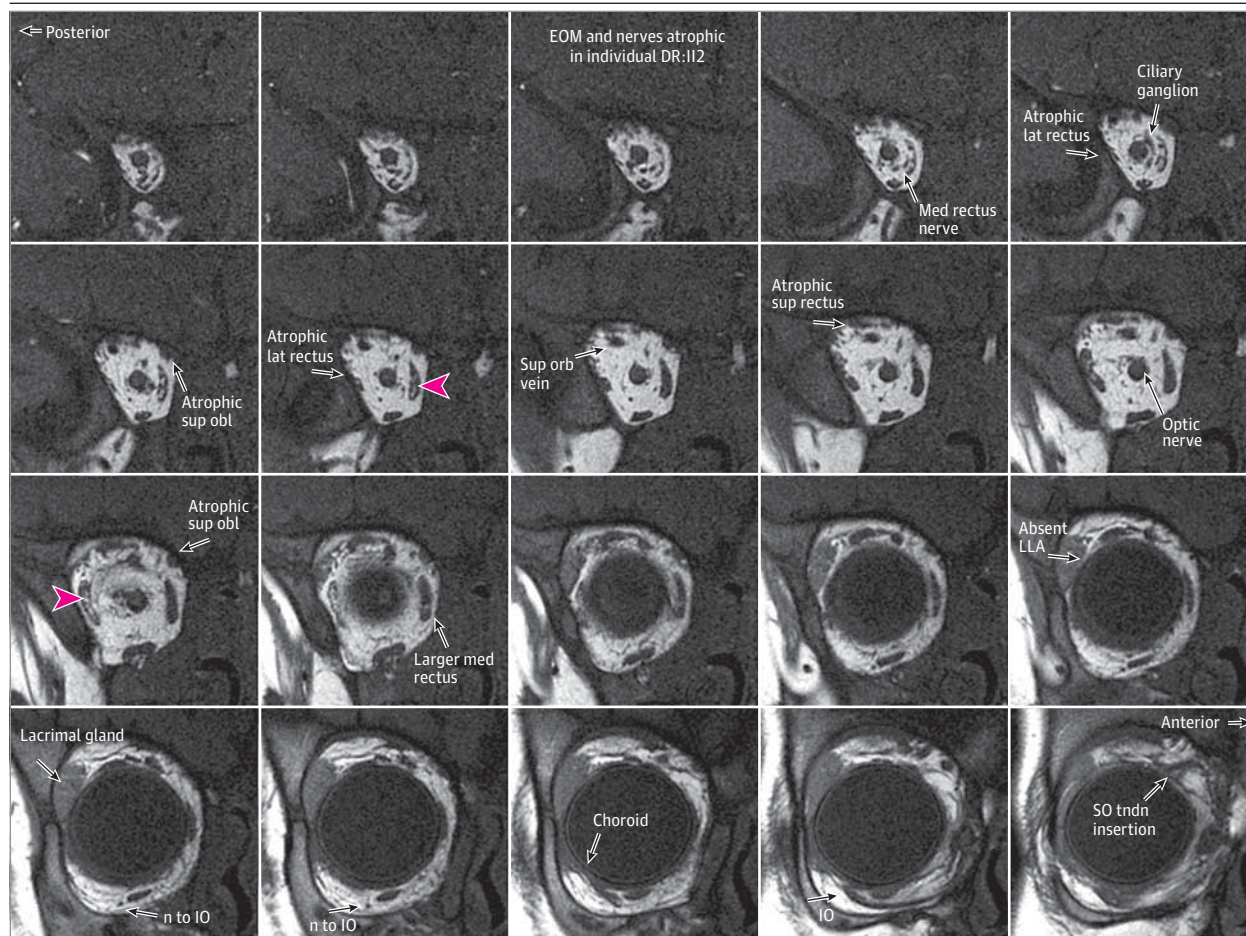
Histochemistry and Electron Microscopy Findings

Histochemistry and electron microscopy of the muscle biopsy specimens from individuals OH IV:1 and DR II:2 revealed nonspecific myopathic changes (Figure 4). Histochemical analysis revealed variability in fiber size, increased endomysial connective tissue, and some internalized nuclei. Type I and type II fibers were observed, with predominance of type I fibers. Multiminicores, central cores, and nemaline rods were not observed. Electron microscopy examination showed similar variation in fiber size with fatty infiltration. Some fibers contained degenerative material with focal accumulation of mitochondria with glycogen and lipid deposition. Focal areas of Z-disc streaming were observed.

Discussion

We studied the affected members of 2 pedigrees diagnosed with atypical Moebius syndrome or congenital fibrosis of extraocular muscles and found them to harbor homozygous or compound heterozygous missense mutations in *RYR1*, leading to

Figure 3. Quasicoronal Magnetic Resonance Imaging of the Right Orbit of Individual DR11:2



Note severe hypoplasia of the lateral (lat) and medial (med) rectus muscles, moderate hypoplasia of the superior (sup) and inferior obliques, and apparent sparing of the inferior rectus. There is central high-intensity material seen within muscles suggestive of fat deposition (red arrowheads). Nerves to the

extraocular muscles (EOM) appear hypoplastic, while the optic nerve, superior orbital vein (Sup orb vein), and intracoronar fat appear normal. IO indicates inferior oblique; LLA, lateral levator aponeurosis; n, nerve; obl, oblique; SO, superior oblique; and tdn, tendon.

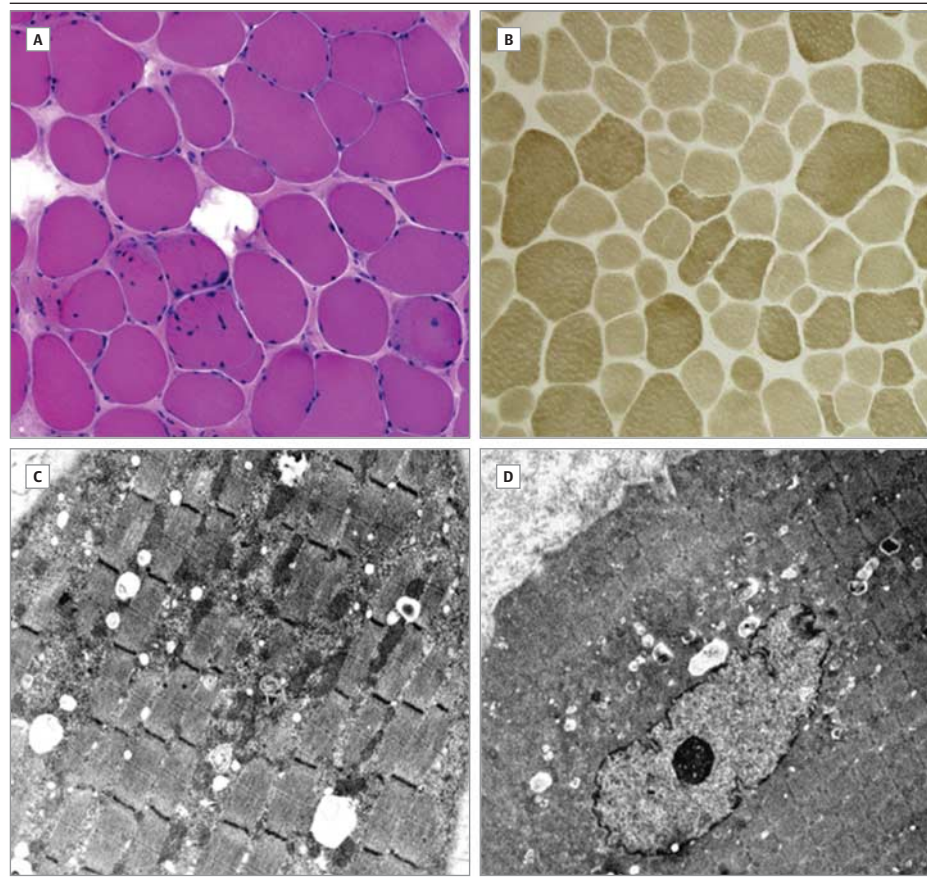
their rediagnosis with *RYR1*-related myopathy with total ophthalmoplegia and susceptibility to malignant hyperthermia. These families highlight *RYR1*-related myopathies in the differential diagnosis of congenital ophthalmoplegia and facial weakness and remind us that risk of malignant hyperthermia can segregate with congenital ophthalmoplegia. They also contribute to the broadening phenotypes associated with *RYR1* mutations. Unlike what is typically found in patients with extraocular muscle involvement and *RYR1* mutations,^{5,6,11,17,34} these patients had relatively mild hypotonia, quite good muscle strength, and no scoliosis or history of respiratory impairment.

We identified the disease-causing mutations in these patients using next-generation exome sequencing, which appears to be a promising diagnostic tool particularly for this disorder. With 106 exons, *RYR1* is expensive and time consuming to Sanger sequence for clinical diagnostics. In addition, *RYR1* mutations cause more than 70% of cases of malignant hyperthermia, which is often inherited as a dominant trait.³⁵ To make a clinical diagnosis of susceptibility to

malignant hyperthermia, a patient must undergo a muscle biopsy and in vitro contracture test, which can yield false-negative results. Thus, exome sequencing can be an important and efficient approach to identify recurrent or novel *RYR1* mutations.

The 3 affected children in pedigree OH harbor 2 different homozygous *RYR1* missense mutations. The first is a novel c.2966 A>G substitution replacing a glutamic acid with a glycine at the highly conserved residue 989. The negative charge of the wild-type residue is lost as a result of this mutation, and this, together with the smaller size of the mutated residue, could disturb the function of *RYR1* or alter its interaction with other molecules.³⁶ The second homozygous mutation is a c.11314C>T substitution replacing an arginine for a tryptophan at residue 3772, which pedigree DR also harbors in the heterozygous state. R3772 is buried within the core of the protein. The pathologic neural tryptophan residue is larger than the negatively charged wild-type arginine residue and thus may disrupt protein-protein interactions within the core structure.

Figure 4. Morphological Findings of Quadriceps Muscle Biopsy Sections From Affected Individual OH IV:1



A, Hematoxylin-eosin stain showing variability of fiber sizes with increased endomysial connective tissue and some internalized nuclei (original magnification $\times 20$). B, Myosin adenine triphosphatase 9.4 stain demonstrating fibers of variable sizes with small type I (light) and II (dark) fibers (original magnification $\times 10$). C and D, Electron micrographs show focal accumulation of mitochondria accompanied by glycogen and lipid droplets (C) (original magnification $\times 4000$), with some fibers showing an internalized nucleus (D) (original magnification $\times 2500$).

In addition to the heterozygous R3772W substitution, the affected dizygotic twins in pedigree DR also harbor a novel heterozygous c.848A>G substitution that replaces a histidine for an arginine at residue 283. The wild-type residue is predicted to form hydrogen bonds with threonine and arginine at positions 286 and 256, respectively, and these bonds are predicted to be disrupted when a neutral histidine is replaced with the larger and positively charged arginine.³⁶

The heterozygous R3772W substitution was previously reported to cause dominantly inherited malignant hyperthermia.³⁷ In our families, it occurs as a recessive mutation in the homozygous or compound heterozygous state and contributes to a broader phenotype that extends beyond susceptibility to malignant hyperthermia. It is interesting that a similar observation was noted for the R3772Q substitution at the same residue: the heterozygous R3772Q substitution was reported to cause malignant hyperthermia,³⁸ while the homozygous or compound heterozygous R3772Q substitution was found to cause a more severe phenotype including ptosis, facial weakness, nonspecific myopathy, and/or malignant hyperthermia.^{37,39,40}

The affected children in pedigree OH harbor 2 homozygous mutations that are both present in their parents in the heterozygous state; thus, both variants are present on the founder allele shared by the 3 parents. Double-variant

mutations in *RYR1* have been reported previously in recessively and dominantly inherited phenotypes,^{17,37,39-42} yet their significance remains controversial. In a study of malignant hyperthermia due to *RYR1* mutations, there was no overt difference in the clinical presentation or muscle response to halothane or caffeine comparing patients with double mutations on the same allele and those with single mutations, except for a significantly higher level of creatinine kinase in the former group.²⁸ On the other hand, as in our report, it appears that when malignant hyperthermia-causing *RYR1* mutations are associated with a second *RYR1* mutation, the resulting phenotype can be more extensive.^{37,40,43} Given these observations, the combination of the homozygous R3772W substitution with the novel homozygous E989G substitution in pedigree OH, or the combination of the heterozygous R3772W substitution with the heterozygous H283R substitution in pedigree DR, could explain the more extensive phenotypes seen in our patients. Moreover, the parents and other family members who harbor heterozygous mutations may, themselves, be at risk of malignant hyperthermia.

It is important for ophthalmologists to consider *RYR1* myopathies in the differential diagnosis of total ophthalmoplegia. Recognizing the clinical associations presented in this report would protect patients and their asymptomatic relatives from the potential risk of malignant hyperthermia.

ARTICLE INFORMATION

Submitted for Publication: January 2, 2013; final revision received March 1, 2013; accepted March 6, 2013.

Published Online: October 3, 2013.
doi:10.1001/jamaophthalmol.2013.4392.

Author Affiliations: Department of Neurology, Boston Children's Hospital, Boston, Massachusetts (Shaaban, Chan, Andrews, Engle); F. B. Kirby Neurobiology Center, Boston Children's Hospital, Boston, Massachusetts (Shaaban, Andrews, Engle); Program in Genomics, Boston Children's Hospital, Boston, Massachusetts (Shaaban, Chan, Engle); Manton Center for Orphan Disease Research, Boston Children's Hospital, Boston, Massachusetts (Shaaban, Engle); Dubai Harvard Foundation for Medical Research, Boston, Massachusetts (Shaaban); Division of Pediatric Neurology, Children's Hospital Los Angeles, Los Angeles, California (Ramos-Platt); Division of Pathology (Neuropathology), Children's Hospital Los Angeles, Los Angeles, California (Gilles); Howard Hughes Medical Institute, Chevy Chase, Maryland (Chan, Andrews, Engle); Department of Pathology, Boston Children's Hospital, Boston, Massachusetts (De Girolami); Department of Pathology, Harvard Medical School, Boston, Massachusetts (De Girolami); Division of Neuropathology, Brigham and Women's Hospital, Boston, Massachusetts (De Girolami); Department of Ophthalmology, Jules Stein Eye Institute, University of California, Los Angeles (Demer); Department of Neurology, Jules Stein Eye Institute, University of California, Los Angeles (Demer); Department of Bioengineering, Jules Stein Eye Institute, University of California, Los Angeles (Demer); Neuroscience Interdepartmental Programs, Jules Stein Eye Institute, University of California, Los Angeles (Demer); Department of Medicine (Genetics), Boston Children's Hospital, Boston, Massachusetts (Engle); Department of Ophthalmology, Boston Children's Hospital, Boston, Massachusetts (Engle); Department of Neurology, Harvard Medical School, Boston, Massachusetts (Engle); Department of Ophthalmology, Harvard Medical School, Boston, Massachusetts (Engle); Broad Institute of MIT and Harvard, Cambridge, Massachusetts (Engle).

Author Contributions: Dr Engle had full access to all of the data in the study and takes responsibility for the integrity of the data and the accuracy of the data analysis.

Study concept and design: Shaaban, Engle.

Acquisition of data: Shaaban, Ramos-Platt, Gilles, Chan, Andrews, De Girolami, Demer.

Analysis and interpretation of data: Shaaban, Ramos-Platt, Demer, Engle.

Drafting of the manuscript: Shaaban, Andrews, Engle.

Critical revision of the manuscript for important intellectual content: Shaaban, Ramos-Platt, Gilles, Chan, De Girolami, Demer, Engle.

Statistical analysis: Shaaban.

Obtained funding: Demer, Engle.

Administrative, technical, or material support: Ramos-Platt, Gilles, Chan, Andrews, Demer.

Study supervision: Demer, Engle.

Conflict of Interest Disclosures: None reported.

Funding/Support: This study was supported by the Al-Habtoor Dubai-Harvard Foundation fellowship (Dr Shaaban), the Manton Center for Orphan

Disease Research (Dr Engle), and National Institutes of Health grants R01EY12498 and R01EY08313. Dr Engle is a Howard Hughes Medical Institute Investigator.

Role of the Sponsor: The funding organizations had no role in the design and conduct of the study; collection, management, analysis, and interpretation of the data; and preparation, review, or approval of the manuscript; and decision to submit the manuscript for publication.

Additional Contributions: We thank the patients and their families who participated in this study. We are grateful to the Broad Institute (funds from the National Human Genome Research Institute grant U54 HG003067, Eric Lander, PhD, principal investigator) and the Ocular Genomics Institute at Massachusetts Eye and Ear Infirmary/Harvard Medical School for generating high-quality sequence data. We also thank Xiaowu Gai, PhD, for help with whole-exome data analysis.

REFERENCES

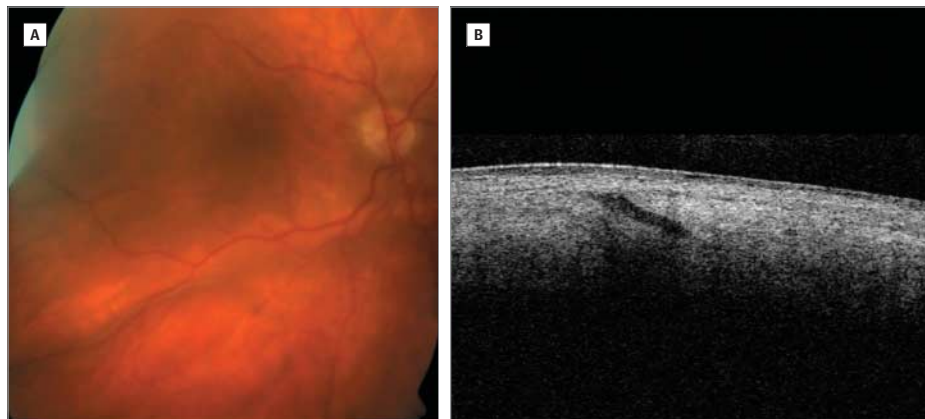
- Lynch PJ, Tong J, Lehane M, et al. A mutation in the transmembrane/luminal domain of the ryanodine receptor is associated with abnormal Ca²⁺ release channel function and severe central core disease. *Proc Natl Acad Sci U S A*. 1999;96(7):4164-4169.
- Monnier N, Romero NB, Lerale J, et al. An autosomal dominant congenital myopathy with cores and rods is associated with a neomutation in the RYR1 gene encoding the skeletal muscle ryanodine receptor. *Hum Mol Genet*. 2000;9(18):2599-2608.
- Monnier N, Romero NB, Lerale J, et al. Familial and sporadic forms of central core disease are associated with mutations in the C-terminal domain of the skeletal muscle ryanodine receptor. *Hum Mol Genet*. 2001;10(22):2581-2592.
- Davis MR, Haan E, Jungbluth H, et al. Principal mutation hotspot for central core disease and related myopathies in the C-terminal transmembrane region of the RYR1 gene. *Neuromuscul Disord*. 2003;13(2):151-157.
- Monnier N, Ferreira A, Marty I, Labarre-Vila A, Mezin P, Lunardi J. A homozygous splicing mutation causing a depletion of skeletal muscle RYR1 is associated with multi-minicore disease congenital myopathy with ophthalmoplegia. *Hum Mol Genet*. 2003;12(10):1171-1178.
- Jungbluth H, Zhou H, Hartley L, et al. Minicore myopathy with ophthalmoplegia caused by mutations in the ryanodine receptor type 1 gene. *Neurology*. 2005;65(12):1930-1935.
- Kondo E, Nishimura T, Kosho T, et al. Recessive RYR1 mutations in a patient with severe congenital nemaline myopathy with ophthalmoplegia identified through massively parallel sequencing. *Am J Med Genet A*. 2012;158A(4):772-778.
- Clarke NF, Waddell LB, Cooper ST, et al. Recessive mutations in RYR1 are a common cause of congenital fiber type disproportion. *Hum Mutat*. 2010;31(7):1544-1550.
- Jungbluth H, Sewry C, Brown SC, et al. Minicore myopathy in children: a clinical and histopathological study of 19 cases. *Neuromuscul Disord*. 2000;10(4-5):264-273.
- Ferreiro A, Estournet B, Chateau D, et al. Multi-minicore disease: searching for boundaries. phenotype analysis of 38 cases. *Ann Neurol*. 2000;48(5):745-757.
- Beggs AH, Agrawal PB. Multiminicore disease. In: Pagon RA, Adam MP, Bird TD, et al, eds. *GeneReviews*. Seattle: University of Washington; 1993.
- MacLennan DH, Duff C, Zorzato F, et al. Ryanodine receptor gene is a candidate for predisposition to malignant hyperthermia. *Nature*. 1990;343(6258):559-561.
- Benkuskuy NA, Farrell EF, Valdivia HH. Ryanodine receptor channelopathies. *Biochem Biophys Res Commun*. 2004;322(4):1280-1285.
- Monnier N, Procaccio V, Stieglitz P, Lunardi J. Malignant-hyperthermia susceptibility is associated with a mutation of the alpha 1-subunit of the human dihydropyridine-sensitive L-type voltage-dependent calcium-channel receptor in skeletal muscle. *Am J Hum Genet*. 1997;60(6):1316-1325.
- Robinson RL, Monnier N, Wolz W, et al. A genome wide search for susceptibility loci in three European malignant hyperthermia pedigrees. *Hum Mol Genet*. 1997;6(6):953-961.
- Strazis KP, Fox AW. Malignant hyperthermia: a review of published cases. *Anesth Analg*. 1993;77(2):297-304.
- Klein A, Lillis S, Munteanu I, et al. Clinical and genetic findings in a large cohort of patients with ryanodine receptor 1 gene-associated myopathies. *Hum Mutat*. 2012;33(6):981-988.
- Dumars S, Andrews C, Chan WM, Engle EC, Demer JL. Magnetic resonance imaging of the endophenotype of a novel familial Möbius-like syndrome. *J AAPOS*. 2008;12(4):381-389.
- Kennedy GC, Matsuzaki H, Dong S, et al. Large-scale genotyping of complex DNA. *Nat Biotechnol*. 2003;21(10):1233-1237.
- Matsuzaki H, Loi H, Dong S, et al. Parallel genotyping of over 10,000 SNPs using a one-primer assay on a high-density oligonucleotide array. *Genome Res*. 2004;14(3):414-425.
- Gudbjartsson DF, Thorvaldsson T, Kong A, Gunnarsson G, Ingólfsson A. Allegro version 2. *Nat Genet*. 2005;37(10):1015-1016.
- Lin M, Wei LJ, Sellers WR, Lieberfarb M, Wong WH, Li C. dChipSNP: significance curve and clustering of SNP-array-based loss-of-heterozygosity data. *Bioinformatics*. 2004;20(8):1233-1240.
- Gnrirke A, Melnikov A, Maguire J, et al. Solution hybrid selection with ultra-long oligonucleotides for massively parallel targeted sequencing. *Nat Biotechnol*. 2009;27(2):182-189.
- Bentley DR, Balasubramanian S, Swerdlow HP, et al. Accurate whole human genome sequencing using reversible terminator chemistry. *Nature*. 2008;456(7218):53-59.
- Wang K, Li M, Hakonarson H. ANNOVAR: functional annotation of genetic variants from high-throughput sequencing data. *Nucleic Acids Res*. 2010;38(16):e164.
- Sherry ST, Ward MH, Kholodov M, et al. dbSNP: the NCBI database of genetic variation. *Nucleic Acids Res*. 2001;29(1):308-311.

27. Abecasis GR, Altshuler D, Auton A, et al; 1000 Genomes Project Consortium. A map of human genome variation from population-scale sequencing [published correction appears in *Nature*. 2011;473(7348):544]. *Nature*. 2010;467(7319):1061-1073.
28. Kumar P, Henikoff S, Ng PC. Predicting the effects of coding non-synonymous variants on protein function using the SIFT algorithm. *Nat Protoc*. 2009;4(7):1073-1081.
29. Adzhubei IA, Schmidt S, Peshkin L, et al. A method and server for predicting damaging missense mutations. *Nat Methods*. 2010;7(4):248-249.
30. Ferrer-Costa C, Gelpí JL, Zamakola L, Parraga I, de la Cruz X, Orozco M. Pmut: a web-based tool for the annotation of pathological mutations on proteins. *Bioinformatics*. 2005;21(14):3176-3178.
31. Li H, Durbin R. Fast and accurate short read alignment with Burrows-Wheeler transform. *Bioinformatics*. 2009;25(14):1754-1760.
32. Li H, Handsaker B, Wysoker A, et al; 1000 Genome Project Data Processing Subgroup. The Sequence Alignment/Map format and SAMtools. *Bioinformatics*. 2009;25(16):2078-2079.
33. Zorzato F, Jungbluth H, Zhou H, Muntoni F, Treves S. Functional effects of mutations identified in patients with multiminicore disease. *IUBMB Life*. 2007;59(1):14-20.
34. Bevilacqua JA, Monnier N, Bitoun M, et al. Recessive RYR1 mutations cause unusual congenital myopathy with prominent nuclear internalization and large areas of myofibrillar disorganization. *Neuropathol Appl Neurobiol*. 2011;37(3):271-284.
35. Rosenberg HSN, Riaz S, Dirksen R. Malignant hyperthermia susceptibility. In: Pagon RA, Adam MP, Bird TD, Dolan CR, Fong CT, Stephens K, eds. *GeneReviews*. Seattle: University of Washington; 2003.
36. Venselaar H, Te Beek TA, Kuipers RK, Hekkelman ML, Vriend G. Protein structure analysis of mutations causing inheritable diseases: an e-Science approach with life scientist friendly interfaces. *BMC Bioinformatics*. 2010;11:548.
37. Levano S, Vukcevic M, Singer M, et al. Increasing the number of diagnostic mutations in malignant hyperthermia. *Hum Mutat*. 2009;30(4):590-598.
38. Carpenter D, Ismail A, Robinson RL, et al. A RYR1 mutation associated with recessive congenital myopathy and dominant malignant hyperthermia in Asian families. *Muscle Nerve*. 2009;40(4):633-639.
39. Kraeva N, Riaz S, Loke J, et al. Ryanodine receptor type 1 gene mutations found in the Canadian malignant hyperthermia population. *Can J Anaesth*. 2011;58(6):504-513.
40. Guis S, Figarella-Branger D, Monnier N, et al. Multiminicore disease in a family susceptible to malignant hyperthermia: histology, in vitro contracture tests, and genetic characterization. *Arch Neurol*. 2004;61(1):106-113.
41. Monnier N, Krivosic-Horber R, Payen JF, et al. Presence of two different genetic traits in malignant hyperthermia families: implication for genetic analysis, diagnosis, and incidence of malignant hyperthermia susceptibility. *Anesthesiology*. 2002;97(5):1067-1074.
42. Romero NB, Monnier N, Viollet L, et al. Dominant and recessive central core disease associated with RYR1 mutations and fetal akinesia. *Brain*. 2003;126(pt 11):2341-2349.
43. Jeong SK, Kim DC, Cho YG, Sunwoo IN, Kim DS. A double mutation of the ryanodine receptor type 1 gene in a malignant hyperthermia family with multiminicore myopathy. *J Clin Neurol*. 2008;4(3):123-130.

OPHTHALMIC IMAGES

Choroidal Detachment Due to Hypotony After Intravitreal Injection of Dexamethasone Implant

Gonzaga Garay-Aramburu, MD; Angela Gomez-Moreno, MD



A, Choroidal detachment in the inferior vascular arcade due to hypotony the day after an intravitreal dexamethasone implant injection. It resolves spontaneously within 4 days. B, Anterior segment optical coherence tomography (Topcon 3D OCT-1000) the day after the injection. The image shows the oblique scleral tunnel open as the cause of hypotony.